

Neurotoxic effects of TDP-43 overexpression in *C. elegans*

Peter E.A. Ash¹, Yong-Jie Zhang¹, Christine M. Roberts², Tassa Saldi², Harald Hutter³, Emanuele Buratti⁴, Leonard Petrucelli¹ and Christopher D. Link^{2,*}

¹Department of Neuroscience, Mayo Clinic College of Medicine, 4500 San Pablo Road, Jacksonville, FL 32224, USA, ²Integrative Physiology/Institute for Behavioral Genetics, University of Colorado, UBC447, Campus Box 447, Boulder, CO 80309, USA, ³Department of Biological Sciences, Simon Fraser University, 8888 University Drive, Burnaby, BC, Canada V5A 1S6 and ⁴Molecular Pathology Group, International Centre for Genetic Engineering and Biotechnology, Trieste, Italy

Received April 1, 2010; Revised May 20, 2010; Accepted June 3, 2010

RNA-binding protein TDP-43 has been associated with multiple neurodegenerative diseases, including amyotrophic lateral sclerosis and frontotemporal lobar dementia. We have engineered pan-neuronal expression of human TDP-43 protein in *Caenorhabditis elegans*, with the goal of generating a convenient *in vivo* model of TDP-43 function and neurotoxicity. Transgenic worms with the neuronal expression of human TDP-43 exhibit an ‘uncoordinated’ phenotype and have abnormal motorneuron synapses. *Caenorhabditis elegans* contains a single putative ortholog of TDP-43, designated TDP-1, which we show can support alternative splicing of CFTR in a cell-based assay. Neuronal overexpression of TDP-1 also results in an uncoordinated phenotype, while genetic deletion of the *tdp-1* gene does not affect movement or alter motorneuron synapses. By using the uncoordinated phenotype as a read-out of TDP-43 overexpression neurotoxicity, we have investigated the contribution of specific TDP-43 domains and subcellular localization to toxicity. Full-length (wild-type) human TDP-43 expressed in *C. elegans* is localized to the nucleus. Deletion of either RNA recognition domain (RRM1 or RRM2) completely blocks neurotoxicity, as does deletion of the C-terminal region. These deleted TDP-43 variants still accumulate in the nucleus, although their subnuclear distribution is altered. Interestingly, fusion of TDP-1 C-terminal sequences to TDP-43 missing its C-terminal domain restores normal subnuclear localization and toxicity in *C. elegans* and CFTR splicing in cell-based assays. Overexpression of wild-type, full-length TDP-43 in mammalian cells (differentiated M17 cells) can also result in cell toxicity. Our results demonstrate that *in vivo* TDP-43 neurotoxicity can result from nuclear activity of overexpressed full-length protein.

INTRODUCTION

The TAR DNA-binding protein (TDP-43) is a ubiquitously expressed, conserved RNA and DNA-binding protein that has been implicated in repression of gene transcription (1), alternative exon splicing (2) and mRNA stability (3). TDP-43 protein has also been identified in ubiquitinated inclusions found in affected neurons in patients with frontotemporal lobar degeneration (FTLD-U) and amyotrophic lateral sclerosis (ALS) (4,5). The consistent deposition of TDP-43 in these diseases, and the identification of TDP-43 mutations in both familial and sporadic forms of ALS,

argues strongly for a causal role for TDP-43 in these neurodegenerative diseases (reviewed in 6). TDP-43-containing inclusions have also been reported in other neurodegenerative conditions, including Alzheimer’s (7) and Parkinson’s disease (8). Consideration of the distribution of TDP-43 in neurodegenerative diseases, and the role of other disease-associated proteins, has led to the proposal that TDP-43 pathology may be primary in the FTLD/ALS spectrum of diseases, but secondary in other neurodegenerative conditions (9).

TDP-43 is an evolutionarily conserved gene, and homologs are found in *Drosophila* and *Caenorhabditis elegans* (10).

*To whom correspondence should be addressed. Tel: +1 3037355112; Fax: +1 3034928063; Email: link@colorado.edu

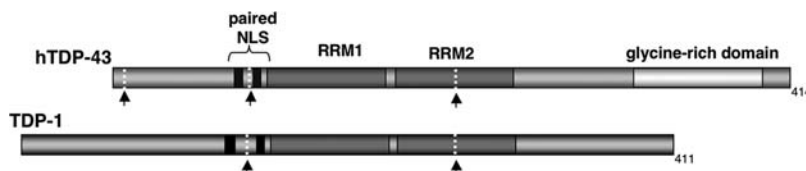


Figure 1. Comparison of hTDP-43 and TDP-1 domain structure. Human TDP-43 and *C. elegans* TDP-1 have similar arrangements of nuclear localization signals, RRM1 and RRM2, and candidate caspase-cleavage sites (arrows). However, TDP-1 lacks an apparent glycine-rich domain and has an extended N-terminus.

The *C. elegans* homolog, designated TDP-1, contains two RNA recognition motifs (RRMs) with a significant sequence similarity to the equivalent domains in TDP-43. TDP-1 also has a nuclear localization signal and similarly positioned caspase-cleavage sites, although it lacks the glycine-rich C-terminal domain of TDP-43 (Fig. 1). We show in the current study that TDP-1 can substitute for TDP-43 in a cell-based CFTR alternative exon splicing assay, supporting the functional orthology of these proteins.

The pathological mechanism(s) associated with TDP-43 deposition are currently unclear. TDP-43 is a predominantly nuclear protein, but in affected ALS motoneurons it is deposited cytoplasmically, with a concurrent reduction in nuclear localization (5). Neuronal nuclear inclusions of TDP-43 have also been observed in FTL-D-U (11). Immunoblot studies of pathological tissue have also demonstrated that cytoplasmic deposition of TDP-43 is associated with the accumulation of C-terminal fragments, most prominently a ~25 kDa species. The existence of putative caspase-cleavage sites in TDP-43 has led to the suggestion that caspase cleavage of TDP-43 may lead to the formation of aggregating C-terminal fragments. Indeed, engineered C-terminal caspase-cleavage fragments of TDP-43 form cytoplasmic aggregates when expressed in cell culture (12). We (13) and others (14) have shown that ectopic expression of C-terminal fragments of TDP-43 leads to the formation of toxic, insoluble, ubiquitin- and phospho-positive cytoplasmic inclusions. However, immunocytochemistry of pathological tissue using antibodies specific for N- and C-terminal TDP-43 epitopes indicates that TDP-43 inclusions can also contain N-terminal portions of this protein, particularly in ALS spinal cord (15).

It is currently unknown whether TDP-43-related pathology is a result of increased, decreased or altered TDP-43 function. ALS-linked TDP-43 mutations appear to act dominantly, consistent with hypermorphic or neomorphic activity of the mutated protein. However, it is also possible that mutant TDP-43 acts in a dominant negative fashion. Studies in cell culture and zebrafish have suggested that both overexpression and loss of TDP-43 function can result in neuronal pathology (16). To broadly investigate the neurotoxic mechanisms of TDP-43 in a genetically tractable model, we have expressed wild-type and mutant forms of human TDP-43 in *C. elegans*, a model system that has previously been used to study a number of human neurodegenerative diseases (17–19). We observe toxicity associated with expression of full-length, nuclearly localized TDP-43, both in *C. elegans* and in cell culture models. In contrast, deletion of the *tdp-1* gene does not cause overt neuronal dysfunction, while transgenic overexpression of TDP-1 does, supporting the

hypothesis that excessive levels of wild-type TDP-43 function is sufficient to induce neuropathology.

RESULTS

To engineer the pan-neuronal expression of human TDP-43 (hTDP-43) in *C. elegans*, a chimeric transgene was constructed in which the promoter region of the *C. elegans* synaptobrevin gene (*snb-1*) drove the expression of a full-length hTDP-43 cDNA. Heritable transgenic strains containing extra-chromosomal copies of the transgenes were generated by microinjection. For a subset of these strains, completely stable transgenic strains containing chromosomally-integrated copies of the transgene were derived by γ -irradiation as previously described (17). All strains containing the *snb-1*/hTDP-43 transgene displayed a distinctive ‘uncoordinated’ (Unc) phenotype typically associated with mutations causing neuronal dysfunction. This uncoordinated phenotype was characterized by non-sinusoidal, slow movement and inappropriate responses to prodding (Fig. 2A and B), as well as a coiled body posture with the dorsal side of the worm on the interior of the coil (i.e. a ‘dorsal coiler’ phenotype). Transgenic worms first display this phenotype as larval animals, and the phenotype remains constant throughout the adulthood. Immunoblot analysis using anti-hTDP-43 antibody demonstrated hTDP-43 expression in the transgenic worms (Fig. 2D), and immunohistochemical staining revealed the accumulation of hTDP-43 specifically in neuronal nuclei (Fig. 2C). We did not observe any anti-ubiquitin staining associated with TDP-43 immunoreactivity or detectable ubiquitin-positive inclusions in these transgenic worms (see Supplementary Material, Fig. S4).

The uncoordinated phenotype observed in the *snb-1*/hTDP-43 transgenic worms is particularly characteristic of *C. elegans* mutants with motoneuron dysfunction. To assay possible motoneuron abnormalities associated with transgene expression, the *snb-1*/hTDP-43 transgene was introduced into a strain containing the *juIs1* reporter transgene (20), which expresses a synaptobrevin::GFP fusion protein under control of *unc-25* promoter. This GFP reporter localizes to GABAergic motoneuron synapses and has been routinely used to visualize these synapses in living worms (21–23). Worms expressing the *snb-1*/hTDP-43 transgene had significant alterations in the number and distribution of synapses tagged by the GFP fusion reporter protein (Fig. 3A and C). Expression of the *snb-1*/hTDP-43 transgene was also associated with occasional axonal defasciculation (observed in 4/30 *snb-1*/hTDP-43 worms, 0/30 controls), visualized by co-expression

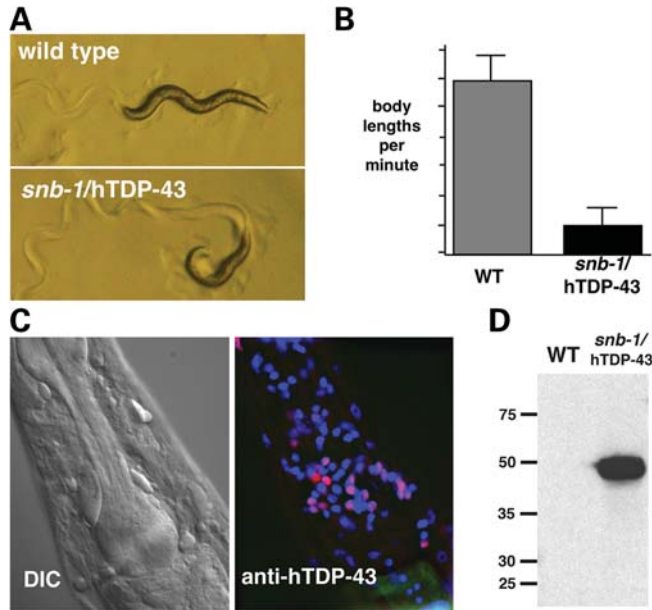


Figure 2. Expression of human TDP-43 in *C. elegans*. (A) Comparison of plate phenotypes for wild-type and *snb-1/hTDP-43* transgenic worms. Note irregular movement tracks and non-sinusoidal body posture of the *snb-1/hTDP-43* worm which is never observed in wild-type animals. (B) Quantification of movement defects in adult *snb-1/hTDP-43* worms (strain CL2609), assayed by measuring total distance traveled for individual worms over 40 s interval. (C) Anterior portion of fixed and permeabilized *snb-1/hTDP-43* worm probed with anti-hTDP-43 antibody (ProteinTech anti-TARDBP polyclonal antibody). Note specific localization of TDP-43 to the nuclei of nerve ring neurons. Red, anti-hTDP-43; blue, DAPI staining of nuclei; green, intestinal GFP from transformation marker plasmid. (D) Immunoblot of extracts from wild-type and *snb-1/hTDP-43* transgenic worms (strain CL1682) probed with anti-TDP-43 monoclonal antibody M01. Note single anti-TDP-43-reactive band in *snb-1/hTDP-43* worms.

of an *rgef-1/DsRed* reporter (Fig. 3B). (In contrast to the synaptic defects, the observed axonal defects are not severe enough to explain the pronounced ‘uncoordinated’ phenotype.)

To determine whether *snb-1/hTDP-43* toxicity was also associated with motorneuron loss, another reporter transgene (*hdlIs22*) was used to specifically tag the 26 GABAergic neurons with DsRed2, including the 19 GABAergic motor neurons. No GABAergic motorneuron loss was observed in fourth larval stage *snb-1/hTDP-43* worms raised at 16°C (Fig. 4A and B). To ask more generally if apoptotic cell death contributes to the uncoordinated phenotype resulting from hTDP-43 expression, the *ced-4(n1162)* mutation was introduced into an *snb-1/hTDP-43* transgenic strain. This mutation in the *ced-4* gene (homologous to mammalian Apaf1) blocks all apoptotic cell death in *C. elegans* (24). Introduction of *ced-4(n1162)* had no effect on the uncoordinated phenotype of fourth larval stage *snb-1/hTDP-43* transgenic worms raised at 16°C, either as observed on agar plates or quantified by counting body thrashes in liquid medium (Fig. 4C).

The uncoordinated phenotype of *snb-1/hTDP-43* worms could be the result of the human TDP-43 protein interfering with the functions of *tdp-1*, the endogenous *C. elegans* ortholog of TDP-43. However, we observed that strains containing *tdp-1* deletions [(*ok781*) or (*ok803*)] have apparently wild-type

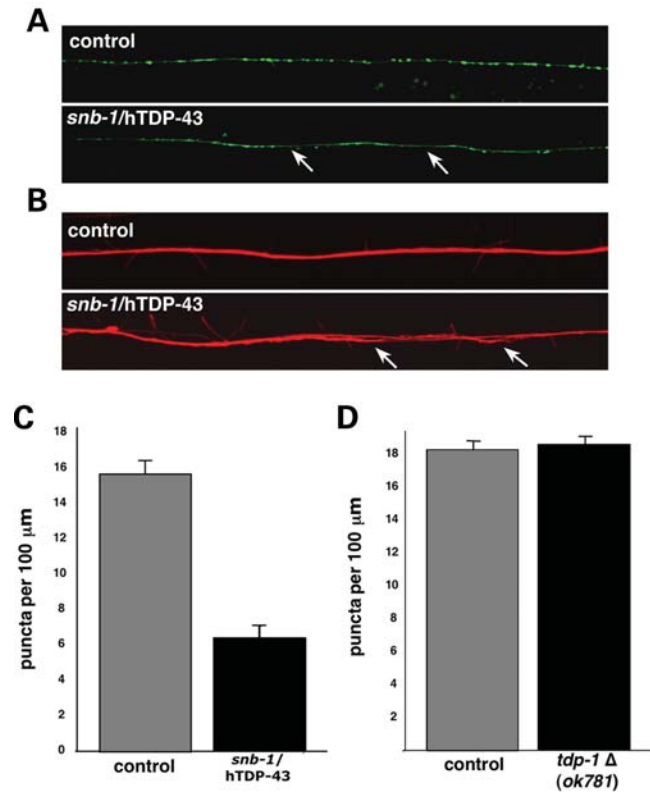


Figure 3. Neuropathology in *snb-1/hTDP-43* transgenic worms. (A) Visualization of GABAergic motor neuron synapses in dorsal cord of living control (CL1685) and *snb-1/hTDP-43* (CL1681) worms using an *unc-25/SNB-1::GFP* reporter transgene (*juls1*). Synapses are visualized as concentrations of the reporter along the axons (‘beads on a string’); note significant reductions in detectable synapses in *snb-1/hTDP-43* worm (arrows). (B) Dorsal cord axonal processes in wild-type and *snb-1/hTDP-43* worms, visualized by co-injection with *rgef-1/DsRed2*, a reporter that accumulates in all axonal processes (40). Note defasciculations in *snb-1/hTDP-43* axonal bundles (arrows). (C) Quantification of dorsal GABAergic synapses in control transgenic (CL1685) and *snb-1/hTDP-43* (CL1681) worms, 30 animals scored for each strain. CL1685, 15.7 ± 0.7 puncta/100 μm; CL1681, 6.5 ± 0.7 puncta/100 μm, Student’s *t*-test $P < 0.0001$. (D) Quantification of dorsal GABAergic synapses in control (*juls1*) and *tdp-1(ok781)*; *juls1* worms, 30 animals scored for each strain. *juls1*, 18.4 ± 0.4 puncta/100 μm; *tdp-1(ok781)*; *juls1*, 18.7 ± 0.4 puncta/100 μm, Student’s *t*-test $P > 0.5$. Error bars = SEM.

movement. To look directly for a role of *tdp-1* in synapse formation, we introduced the *juls1* reporter into a *tdp-1(ok781)* background and scored GABAergic synapses as described above (Fig. 3D). No synaptic abnormalities were observed in the *tdp-1* deletion background, indicating that the effects of the *snb-1/hTDP-43* transgene are unlikely to be due to a direct dominant negative interaction between hTDP-43 and TDP-1. Introduction of *tdp-1(ok781)* into the transgenic *snb-1/hTDP-43* background did not modify the *snb-1/hTDP-43* uncoordinated phenotype (Fig. 4C), indicating that the toxicity of hTDP-43 also does not depend upon interaction with endogenous TDP-1.

The observations described above could be explained if human TDP-43 was a functional homolog of TDP-1 and excess expression of TDP-1 activity was sufficient to induce neuronal dysfunction. However, initial reports using *in vitro*

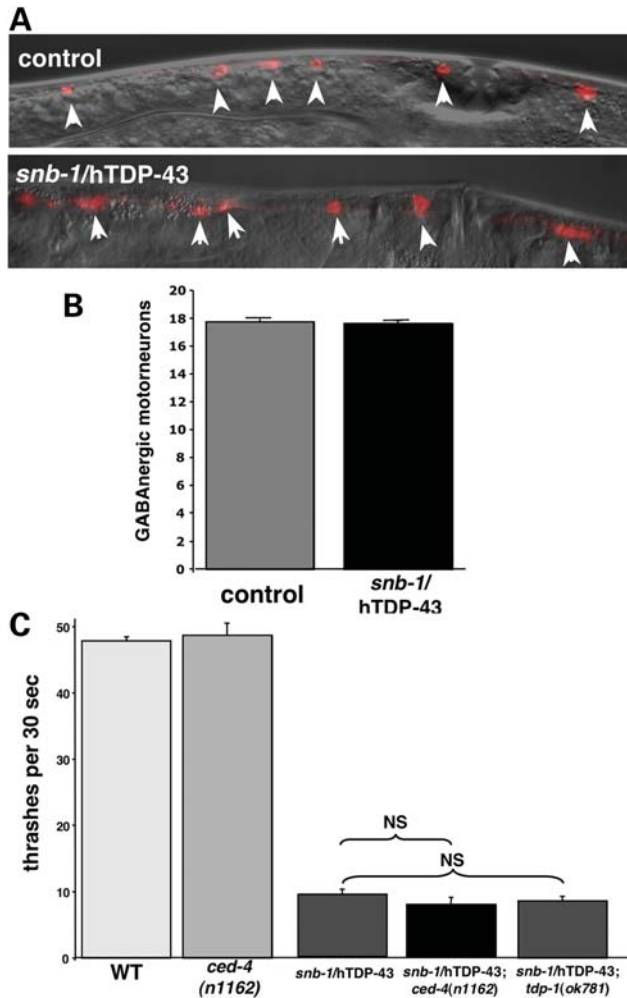


Figure 4. The uncoordinated phenotype induced by *snb-1/hTDP-43* is not associated with neuronal loss. (A) Visualization of GABAergic motor neurons using *unc-47/DsRed2* reporter transgene (*hds22*). (B) Quantification of GABAergic motor neurons in control and *snb-1/hTDP-43* worms, 30 animals scored for each strain. *hds22* control, 17.6 ± 0.2 GABAergic motorneurons per worm; *hds22; snb-1/hTDP-43*, 17.7 ± 0.2 GABAergic motorneurons per worm, Student's *t*-test $P > 0.5$. (C) Effect of *ced-4(n1162)* and *tdp-1(ok781)* on movement in liquid in *snb-1/hTDP-43* worms. *ced-4(n1162)* does not influence the movement in non-transgenic [wild-type, 47.8 ± 0.6 thrashes/30 s; *ced-4(n1162)*, 48.7 ± 1.8 thrashes/30 s, Student's *t*-test $P > 0.5$] or transgenic [*snb-1/hTDP-43*, 9.4 ± 0.8 thrashes/30 s; *ced-4(n1162); snb-1/hTDP-43*, 7.9 ± 1.1 thrashes/30 s, Student's *t*-test $P > 0.2$] worms. Similarly, introduction of the *tdp-1(ok781)* deletion into the *snb-1/hTDP-43* background does not alter the reduced movement caused by this transgene [*snb-1/hTDP-43*, 9.4 ± 0.8 thrashes/30 s; *tdp-1(ok781); snb-1/hTDP-43*, 8.3 ± 0.5 thrashes/30 s, Student's *t*-test $P > 0.1$]. Error bars = SEM.

assays indicated that TDP-1 could not substitute for TDP-43 in alternative splicing of CFTR transcripts (10), raising questions about the functional orthology of these proteins. We therefore re-examined the ability of TDP-1 to support alternative splicing of CFTR in a cell-based system. Employing HeLa cells, we expressed a CFTR reporter minigene construct with a C155T exon 9 mutation (Fig. 5A) that has previously been shown to produce inhibition of exon 9 inclusion under control of endogenous HeLa TDP-43 (37). Under these conditions, knockdown of TDP-43 rules out any potential interactions of

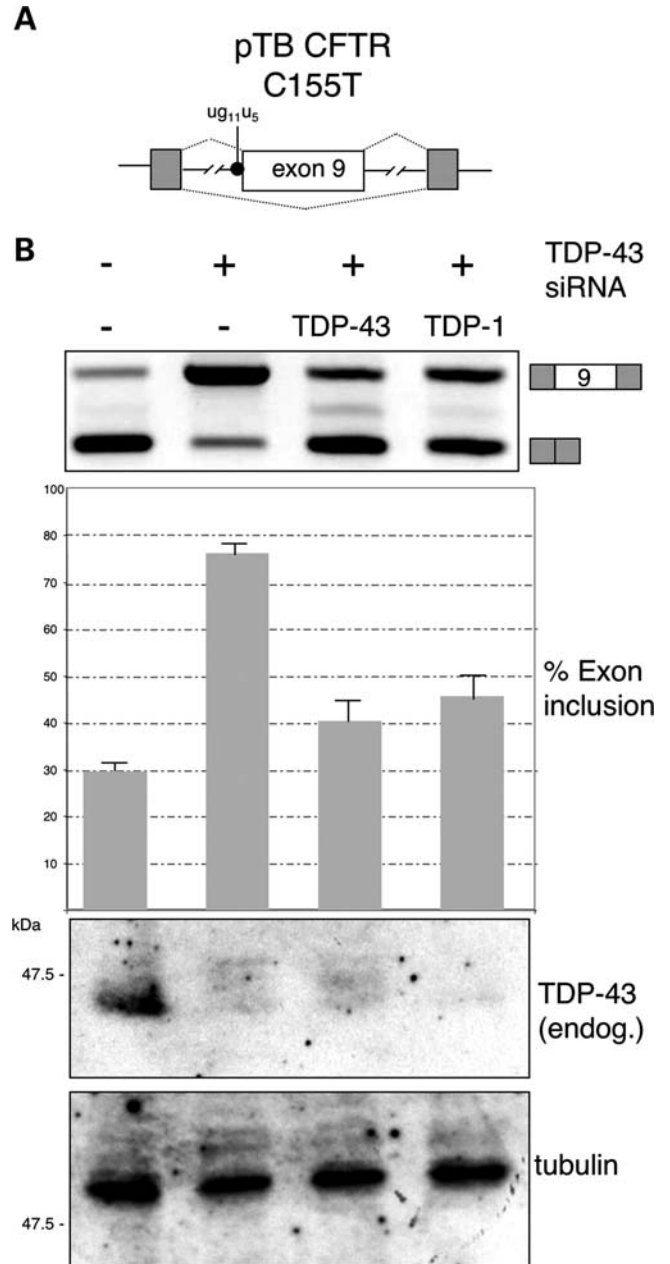


Figure 5. TDP-1 can promote CFTR alternative splicing in a cell-based assay. (A) Schematic diagram of the CFTR C155T minigene transfected in add-back assay (dotted lines represent possible splicing outcomes). (B) Effect on CFTR exon 9 splicing of adding back siRNA-resistant wild-type human TDP-43 and TDP-1 following knockdown of the endogenous TDP-43. Standard deviations obtained in three independent transfection experiments are shown. The western blots against the endogenous TDP-43 and tubulin are shown in the lower boxes to show silencing efficiency and equal loading. The weak immunoblot signal from the transfected siRNA-resistant TDP-43 is likely due to the relatively low transfection efficiency of this plasmid construct (37).

the endogenous protein and allows the direct assessment of the functional ability of the reintroduced siRNA-resistant constructs to inhibit the inclusion of exon 9 from the CFTR transcript. As shown in Figure 5, TDP-1 can support CFTR splicing in this system, strengthening the functional similarities between TDP-43 and TDP-1.

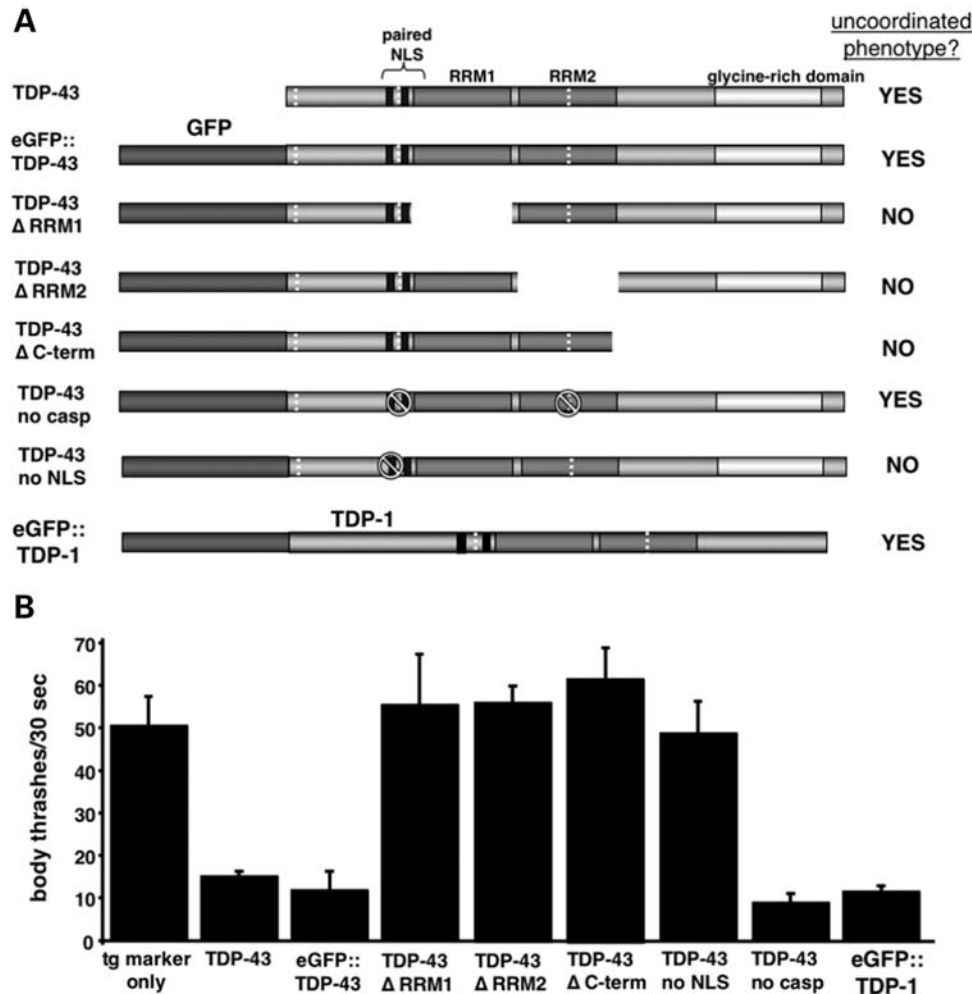


Figure 6. Neurotoxicity of engineered TDP-43 variants expressed in *C. elegans*. (A) Schematic representation of TDP-43 variants expressed in *C. elegans*. (B) Quantification of movement defects induced by the expression of wild-type or variant TDP-43. Transgenic worms expressing wild-type TDP-43 (strain CL1682), eGFP::TDP-43 (strain CL1626), TDP-43 caspase site mutant (strain CL1690) or eGFP::TDP-1 (strain LEN144) all show significantly reduced body thrashes in liquid in comparison to control transgenic worms expressing a marker transgene only (strain CL1685) ($P < 0.001$, Student's *t*-test). In contrast, transgenic worms expressing eGFP::TDP-43 with a deletion of RRM1 (strain CL1702), RRM2 (strain CL1705) or the C-terminus (strain CL1710) do not have reduced body thrash rates (*t*-test $P > 0.2$). Mutation of the nuclear localization signal in an eGFP::TDP-43 construct (strain CL1687) similarly restores body movement to control levels. All strains were assayed at 16°C, except LEN144, which was assayed at 25°C to maximize transgene expression. Error bars = SEM.

To investigate whether excessive TDP-1 expression could in fact cause neuronal dysfunction, we generated parallel transgenic strains in which the *snb-1* promoter drove the expression of a TDP-1 cDNA (in a background with endogenous *tdp-1* expression). These transgenic strains also employed a temperature-sensitive mutation in the *smg-1* gene that allows levels transgene expression to be moderated by growth temperature (25). At higher temperatures (higher transgene expression, see Supplementary Material, Fig. S1), *snb-1*/eGFP::TDP-1 transgenic worms displayed an uncoordinated phenotype and reduced movement in the thrashing assay (see Fig. 6B). We therefore postulate that human TDP-43 neurotoxicity in *C. elegans* may result from excess (wild-type) TDP-43 function.

Next we sought to determine which domains of hTDP-43 were required for induction of neurotoxicity in *C. elegans*. The TDP-43 protein contains two RRMs (RRM1 and RRM2), nuclear localization and export signals, and a

C-terminal glycine-rich domain. RRM1 is both necessary and sufficient for nucleotide binding (2), and the glycine-rich domain has been reported to be responsible for the interaction of TDP-43 with heterogeneous nuclear ribonucleoproteins (hnRNPs), in particular hnRNP A2/B1 and hnRNP A1 (26). In this series of experiments, wild-type and deletion variants of hTDP-43 included N-terminal GFP fusions to allow rapid confirmation of transgene expression and determination of the subcellular localization of the expressed fusion protein in live worms. Schematics of these constructions are shown in Figure 6A. Expression of the appropriate fusion construct was confirmed by immunohistochemistry and immunoblotting (see Supplementary Material, Fig. S2) and effects of transgene expression on motility was assayed using the thrashing assay. Neuronal expression of a GFP::hTDP-43 (full-length) fusion protein resulted in an uncoordinated phenotype and nuclear accumulation of the transgenic product indistinguishable from that observed in worms expressing untagged hTDP-43.

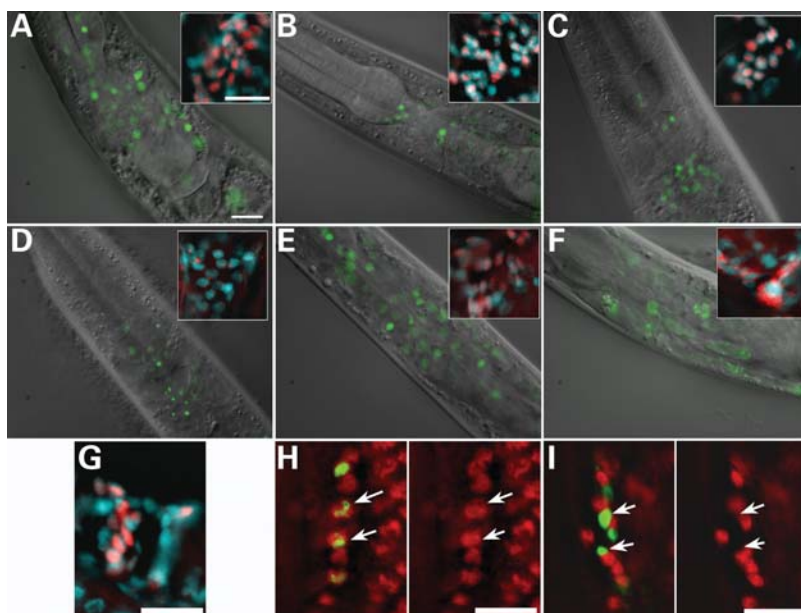


Figure 7. Localization of *snb-1*-driven full-length and variant hTDP-43 constructs expressed in *C. elegans*. (A–F) Fused GFP/DIC images of live transgenic worms expressing eGFP::TDP-43 fusions (main panel), with complementary inserts of the nerve ring area of a fixed worm from the same transgenic strain probed with anti-TDP-43 antibody (red) and counter-stained with DAPI (blue) to highlight nuclei. (A) Nerve ring area of eGFP::hTDP-43 transgenic worm (CL1626). GFP fluorescence and anti-TDP-43 staining were localized to nuclei and were primarily diffuse in the nucleus. (B) Nerve ring area of eGFP::hTDP-43 RRM1 deletion transgenic worm (CL1702). GFP fluorescence and anti-TDP-43 staining were nuclear but more punctate than observed for full-length eGFP::hTDP-43. (C) Nerve ring area of eGFP::hTDP-43 RRM2 deletion transgenic worm (CL1705). GFP fluorescence and anti-TDP-43 staining were nuclear but also somewhat more punctate than observed for full-length eGFP::hTDP-43. (D) Nerve ring area of eGFP::hTDP-43 C-terminal deletion (i.e. hTDP-43 1–257, strain CL1710). GFP fluorescence and anti-TDP-43 staining were localized to a single nuclear body/inclusion in most neurons. (E) Nerve ring area of eGFP::hTDP-43 no caspase-cleavage (D89E, D219E) mutant transgenic worm (CL1690). As observed for the eGFP::hTDP-43 (wild-type) fusion (A), GFP fluorescence and anti-TDP-43 staining were localized to nuclei and were primarily diffuse in the nucleus. (F) Nerve ring area of eGFP::hTDP-43 NLS1 mutant transgenic worm (strain CL1687). GFP fluorescence and anti-TDP-43 staining were observed in both perinuclear cytoplasmic inclusions and diffusely in the cytoplasm. (G) Nerve ring area of fixed worm expressing an hTDP-43::TDP-1 fusion construct (CL1714), probed with anti-hTDP-43 monoclonal antibody (red) and DAPI (blue). Addition of C-terminal TDP-1 sequences restored diffuse nuclear distribution to this hTDP-43 variant, which is normally lost when hTDP-43 C-terminal sequences are deleted (compare with D inset). (H) Ventral cord region of fixed eGFP::hTDP-43 transgenic worm (CL1626) (GFP in green, DAPI staining, false-colored red). The fusion protein shows strict nuclear localization, as illustrated by comparison of GFP + DAPI (left) and DAPI only (right) images (arrows). (I) Ventral cord region of fixed eGFP::hTDP-25 F1 transgenic worm (GFP in green, DAPI staining false, colored red). The fusion protein forms large inclusions with strict cytoplasmic localization, as illustrated by comparison of GFP + DAPI (left) and DAPI only (right) images (arrows). Size bar = 10 μ m in all images.

In contrast, expression of fusions containing deletions of either the first RRM (RRM1, residues 106–175) or the second RRM (RRM2, residues 193–257) did not result in uncoordinated movement. Similarly, the expression of a GFP fusion protein containing a deletion of the hTDP-43 C-terminal region (residues 257–414) failed to induce the uncoordinated phenotype. Quantification of movement phenotypes in the TDP-43 deletion variants is shown in Figure 6B.

Although all of these deletion variants retained their nuclear localization, the subnuclear distribution of the variants appeared different from that of the full-length fusion protein (Fig. 7A). The RRM1 and RRM2 deletion proteins had a more granular appearance, and the C-terminal deletion protein was localized to a singular nuclear body or inclusion (Fig. 7B–D). The cellular distribution of these TDP-43 variants was clearly different from that of GFP fused to a C-terminal TDP-43 fragment (eGFP::TDP-25), which, as previously observed in cell culture (12), produced only large cytoplasmic aggregates (Fig. 7I). Interestingly, fusion of a TDP-1 C-terminal domain (residues 347–411) to the TDP43 N-terminal domain (residues 1–269) restored the normal

nuclear distribution lost when the TDP-43 C-terminus was deleted (compare Fig. 7G and D inset).

The ability of TDP-1 C-terminal sequences to restore normal nuclear localization to C-terminally deleted TDP-43 raised the question of whether addition of the C-terminal TDP-1 sequences could similarly restore TDP-43 function. We therefore examined the ability of TDP-1 C-terminal sequences to rescue CFTR alternative splicing lost when the TDP-43 C-terminal sequences are deleted (2). As shown in Figure 8A–C, we found that whereas TDP-43 N-terminal sequences could not support alternative splicing of CFTR, the TDP-43(N-terminal)::TDP-1(C-terminal) construct robustly supported exon exclusion in this cell-based assay. Furthermore, addition of the TDP-1 C-terminal sequences to N-terminal TDP-43 restored normal nuclear localization (Supplementary Material, Fig. S3), as observed in the *C. elegans* model. As predicted, the TDP-43::TDP-1 fusion construct was also neurotoxic in *C. elegans* (Fig. 8D).

In all transgenic strains examined, full-length hTDP-43 could only be detected in nuclei, either by GFP tagging or by immunohistochemistry. However, these experiments do not exclude the possibility that the observed neurotoxicity could result

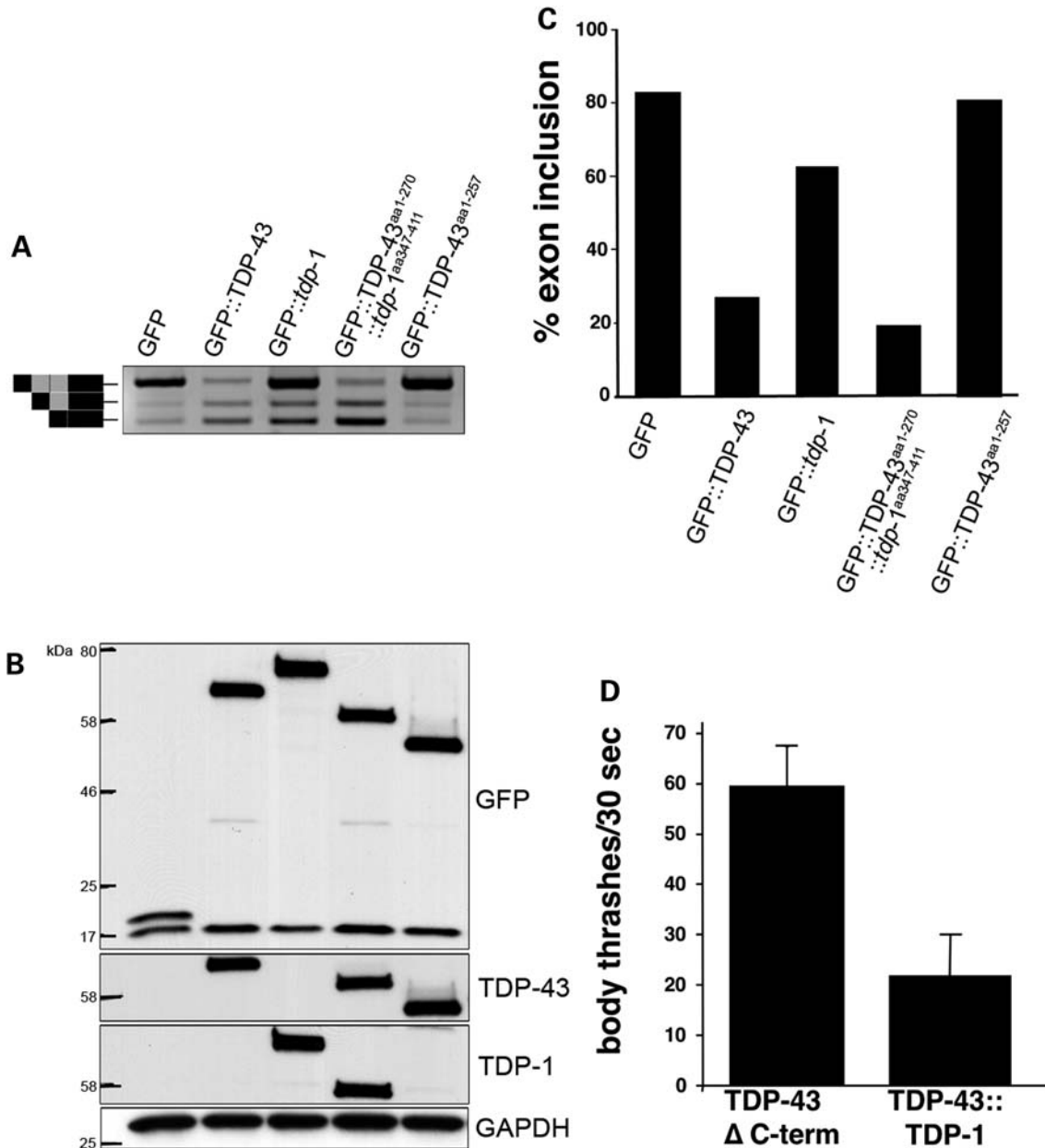


Figure 8. Activity of TDP-43 deletion and fusion proteins. (A) cDNA prepared from co-transfected cells was used as a template for PCR to determine relative exclusion of CFTR exon 9 from the (TG)₁₃(T)₅ minigene. (B) Immunoblot using (rabbit) anti-GFP (Invitrogen) to probe for tagged construct expression. Loading controlled for using (mouse) anti-GAPDH (BioDesign). (C) Desitometric readings from CFTR minigene PCR (A) were used to determine the percent inclusion of exon 9 in CFTR minigene for each sample. [In contrast to the pTB CFTR C155T minigene used in Figure 5A, the (TG)₁₃(T)₅ CFTR construct used to assess the function of the TDP-43^{aa1-270}::TDP-1^{aa347-411} fusion construct lacks the C155T CFTR mutation. Under control of endogenous TDP-43 the (TG)₁₃(T)₅ minigene is more resistant to inhibition of exon 9 inclusion and requires overexpression of TDP-43 to induce exon 9 skipping (13), providing a rigorous test of the ability of the TDP-43::TDP-1 fusion to promote exon skipping.] (D) Effect of TDP-43::TDP-1 fusion protein on impaired body movement in *C. elegans*. Transgenic worms containing an addition of TDP-1 C-terminal sequences to the TDP-43 N-terminus have a significant decrease in body movement ($P < 0.01$, Student's *t*-test).

from the production of low levels of undetectable (but highly toxic) cytoplasmic C-terminal fragments, perhaps by cleavage of endogenous *C. elegans* caspases. We therefore expressed full-length TDP-43 containing substitutions (D89E, D219E) that block caspase cleavage and prevent the formation of C-terminal TDP-43 fragments in cell culture experiments (12). Expression of the caspase-cleavage-insensitive hTDP-43

still resulted in uncoordinated transgenic worms, indicating that hTDP-43 toxicity does not require caspase cleavage (Fig. 6B). This result is consistent with the inability of the *ced-4(n1162)* mutation, which blocks caspase activation in *C. elegans*, to reverse hTDP-43 toxicity. To rigorously demonstrate that nuclear, not cytoplasmic, full-length hTDP-43 is toxic, we expressed hTDP-43 containing substitutions (K82S,

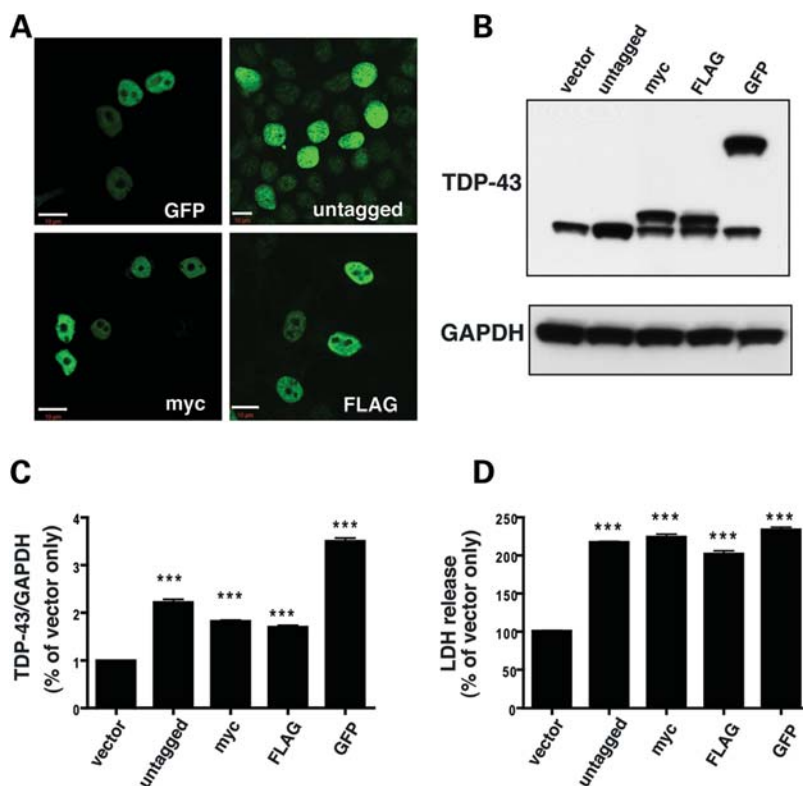


Figure 9. Toxicity of full-length hTDP-43 in mammalian cell culture. Differentiated M17 cells were transfected for 72 h with 1 μg of constructs expressing either wild-type or tagged full-length hTDP-43. (A) Visualization of cellular distributions of transfected proteins. Top left panel, GFP fluorescence; top right panel, anti-TDP-43 (ProteinTech polyclonal antibody) immunofluorescence; bottom left panel, anti-myc immunofluorescence; bottom right panel, anti-FLAG immunofluorescence. All detected transfected protein expression was nuclear. Size bar = 10 μm. (B) TDP-43 expression levels of transfected cells measured by immunoblot (polyclonal anti-TDP-43 antibody, ProteinTech). (C) Densitometric analysis of immunoblot shown in (B). Note transfected cells express ~2–3-fold more TDP-43 than control transfected cells. (D) Cell toxicity of TDP-43 overexpression assayed by LDH release. LDH release was significantly higher in cells transfected with TDP-43 constructs than in control vector-transfected cells. Data from three separate experiments were analyzed by one-way analysis of variance followed by Tukey's *post hoc* analysis. (***) $P < 0.001$.

R83S, K84S) that inactivated NLS1 of the bipartite NLS. This hTDP-variant was strictly cytoplasmic, with TDP-43 being distributed both diffusely and in small inclusions (Fig. 7F). Transgenic animals expressing NLS-mutated hTDP-43 were not uncoordinated, despite expressing levels of TDP-43 comparable to those of wild-type hTDP-43 strains (Supplementary Material, Fig. S2) that show clear neurotoxicity. These results support the view that nuclear, full-length TDP-43 is a toxic species in this *C. elegans* model.

To determine whether this toxicity of full-length TDP-43 could also be observed in mammalian cells, we transfected TDP-43 (untagged or containing myc, FLAG or GFP tags) into differentiated M17 cells. All detectable transfected hTDP-43 appeared nuclear (Fig. 9A). The transfected cells contained ~2–3-fold more TDP-43 than the endogenous TDP-43 measured in control vector-transfected cells (Fig. 9B and C). Despite this relatively modest overexpression of TDP-43, and the absence of TDP-43 C-terminal fragments detectable by immunoblot, TDP-43 transfected cells showed a significant decrease in viability as measured by increased LDH release (Fig. 9D). These observations indicate that overexpression of wild-type, full-length TDP-43 can have toxic effects in a mammalian cell culture model.

DISCUSSION

We have demonstrated that wild-type human TDP-43 can be toxic when expressed in a heterologous *C. elegans* system or overexpressed in a cell culture model. The neurotoxicity of hTDP-43 in *C. elegans* depends on the nuclear accumulation of the full-length protein. It is unlikely that the neurotoxicity of hTDP-43 is due to non-specific effects of expression of a heterologous protein, as we have used the identical expression system to express GFP (27) and the β-amyloid peptide (28) without observing the dramatic uncoordinated phenotype seen in hTDP-43 transgenic worms. The observation that hTDP-43 toxicity requires both RNA recognition domains further demonstrates the specificity of hTDP-43 toxicity and is consistent with the hypothesis that this toxicity requires interaction with either DNA or RNA.

We find that the uncoordinated phenotype of hTDP-43 transgenic worms is correlated with abnormal motor neuron synapses. Although we have not assayed for other neuronal deficits, *C. elegans* mutations that cause dysfunction specifically in the GABAergic neurons assayed in our study are sufficient to induce an uncoordinated phenotype (29). Interestingly, we did not detect a loss of GABAergic motor

neurons in hTDP-43 transgenic worms (although we have not scored these neurons in aged transgenic worms or in transgenic worms under stressful conditions). Motor neuron cell loss is observed in the spinal cord of ALS patients, although it is unclear whether this is due to a direct activation of cell death pathways or secondary to synaptic and axonal loss. In a mouse ALS model expressing G93A mutant SOD1, introduction of a *bax* deletion could disassociate motor neuron death from motor neuron dysfunction, suggesting that clinical symptoms in this model result from damage to distal motor neuron axons, not direct activation of cell death pathways (30). Although we have only directly assayed a limited population of neurons for cell loss, introduction of a *ced-4(n1162)* mutation that blocks all programmed cell death of *C. elegans* neurons [analogous to the *bax* deletion experiment described in Gould *et al.* (30)] failed to suppress the uncoordinated phenotype resulting from hTDP-43 expression. Results in this *C. elegans* model are therefore consistent with TDP-43 toxicity also acting primarily by inducing motor neuron axonal/synaptic dysfunction, not by direct activation of a cell death pathway. This is consistent with our previous mammalian cell culture experiments (13).

We have used cell transfection experiments to demonstrate in HeLa cells that after siRNA knockdown of endogenous TDP-43, transfected TDP-1 can support alternative splicing of a CFTR reporter construct. It also appears that C-terminal TDP-1 sequences can restore splicing function and appropriate nuclear localization to C-terminally deleted TDP-43. In addition to supporting the orthology of TDP-43 and TDP-1, these observations raise questions regarding the function of the TDP-43 C-terminus. There is no apparent sequence similarity between the TDP-43 and TDP-1 C-terminal regions, and TDP-1 does not have an apparent glycine-rich domain (10). While it is possible that the TDP-1 C-terminus nevertheless interacts with the same hnRNPs as does the TDP-43 C-terminus (26), an alternative interpretation for the ability of the TDP-1 C-terminus to substitute for the TDP-43 C-terminus in the splicing assay is that any sequences capable of correcting the nuclear localization defect of C-terminally deleted TDP-43 may be able to similarly rescue alternative splicing in cell-based assays.

Expression of hTDP-43 containing a deletion of RRM1 did not lead to detectable toxicity but altered the subnuclear distribution of TDP-43. This nuclear redistribution of TDP-43 appears very similar to that observed for RRM1-deleted hTDP-43 expressed in U2OS cells (31). Deletion of RRM2 also blocked TDP-43 toxicity and resulted in nuclear redistribution of the transgenic protein. This nuclear redistribution of hTDP-43 RRM deletion variants may reflect the association of the variants with a different subnuclear domain, although we are currently unable to test this directly due to the lack of appropriate *C. elegans* antibodies. Deletion of the hTDP-43 C-terminus dramatically changed hTDP-43 nuclear localization, with a single TDP-43 inclusion typically visible in the nucleus (Fig. 7D). Ayala *et al.* (31) also reported C-terminal deletions of hTDP-43 forming inclusions in cell culture; however, these inclusions were variable and observed both in the cytoplasm and in the nucleus.

The toxicity of wild-type and deletion variants of hTDP-43 has also been assayed in yeast by high-level expression of progressive N- and C-terminal deletion constructs (32). These researchers

observed toxicity of full-length and C-terminal hTDP-43 in this model. Although these researchers attributed the toxicity of full-length hTDP-43 to cytoplasmic accumulation, our evidence strongly supports nuclear full-length hTDP-43 being toxic in both the *C. elegans* and cell culture models. This discrepancy could result because yeast lack an apparent TDP-43 ortholog (and possibly some TDP-43-dependent processes).

We have also found that *C. elegans* expression of hTDP-43 containing point mutations in NLS1 result in cytoplasmic accumulation of both diffuse and aggregated hTDP-43. In contrast to cytoplasmic aggregates formed by a C-terminal hTDP-43 fragment (13), full-length cytoplasmic hTDP-43 aggregates do not appear to be neurotoxic in this *C. elegans* model. This result supports the view that C-terminal hTDP-43 fragments have a novel gain of function associated with their toxicity. This result also supports the contention that nuclear localization of TDP-43 is specifically required for the neurotoxicity we see in this model. The mechanism(s) by which nuclear TDP-43 activity leads to abnormal synapses is unknown, but a plausible explanation is that excessive TDP-43 activity alters some component of RNA metabolism (e.g. alternative splicing), subsequently leading to altered production of specific proteins required for proper synaptic function.

An important unanswered question is whether overexpression of (wild-type) TDP-43 activity plays a role in human neurodegenerative diseases. Much evidence points to an association between accumulation of C-terminal hTDP-43 fragments and neurodegeneration; as these fragments do not appear to be functional (13), the mechanism of their toxicity is unlikely to be the same as we have demonstrated for full-length hTDP-43 in *C. elegans* or cell culture. However, it is plausible that a dysregulation of wild-type TDP-43 function plays a central role in neurodegenerative disease, with the production of C-terminal TDP-43 fragments an attempt by neurons to counter excess TDP-43 function. Expression of wild-type hTDP-43 in *Drosophila* has recently been shown to induce neurotoxicity (33), and two groups have also recently reported the engineering of transgenic mice expressing hTDP-43, either wild-type (34) or ALS mutant [hTDP-43 Ala³¹⁵Thr (35)]. Interestingly, in the fly model, eye-specific expression of a TDP-43 N-terminal deletion variant lacking the RRM domains also failed to produce detectable neurotoxicity. In both mouse models, transgenic mice had neuropathological phenotypes reminiscent of FTL/ALS and accumulation of C-terminal hTDP-43 fragments. Although cytoplasmic ubiquitinated inclusions were observed in both models, TDP-43 was either absent from these inclusions (in ALS mutant TDP-43 mice) or present in a subpopulation (wild-type TDP-43 mice). Thus, as observed in *C. elegans*, these transgenic models demonstrate that overexpression of wild-type hTDP-43 can be neurotoxic, and this toxicity does not require cytoplasmic deposition of hTDP-43.

The primary rationale for developing a transgenic *C. elegans* TDP-43 model is the potential to use genetic approaches to investigate TDP-43 functions and mechanisms of toxicity. We have recently identified mutations that suppress neuronal deficits in hTDP-43 transgenic worms (unpublished data), and anticipate that characterization of these mutations will minimally give us insight into TDP-43

functions, and potentially reveal neurotoxic mechanisms relevant to human disease.

MATERIALS AND METHODS

Transgene construction

All *C. elegans* transgene constructs were derived from pan-neuronal expression vector pCL35, which contains promoter sequences from the *C. elegans* synaptobrevin (*snb-1*) gene (36). This construct also contains an extended 3'-untranslated region that can convey temperature-sensitive expression levels when transgenes are introduced into a *smg-1(cc546ts)* mutant background (25). Expression of wild-type human TDP-43 was engineered by cloning a full-length TDP-43 cDNA sequence into the *XbaI/BamHI* sites in the multiple cloning site of pCL35. Expression of variant TDP-43 sequences was engineered by recovering the relevant sequences from mammalian expression constructs and cloning these into the *XhoI/XbaI* sites of pCL35. TDP-1 expression was similarly engineered using full-length TDP-1 cDNA cloned from *C. elegans* wild-type strain N2. Residue numbering for the TDP-1 constructs is based on the F44G4.4a splice variant (Wormbase). See Supplementary Material for construction details.

Transgenic strain construction

Transgenic *C. elegans* strains were generated by gonad micro-injection of plasmid DNA containing the construct of interest paired with an independent transformation marker plasmid. For clarity, we have used the convention that transgenes generated by transcriptional fusions to *C. elegans* promoters are identified with a '/' (e.g. *snb-1/hTDP-43*), whereas translational fusions are indicated using the '::' convention (e.g. GFP::hTDP-43). Marker plasmids used were: pRF4 [dominant Roller morphological marker gene *rol-6(su1006)*]; pCL26 (*mtl-2/GFP*, constitutive intestinal GFP); pVH13.06 (*rgef-1/DsRed2*, pan-neuronal DsRed) and *unc-122/GFP* (coelomocyte GFP). (Full-length hTDP-43 induced the uncoordinated phenotype when co-injected with any of the transformation markers.) Transgenic strains generated in this manner have heritable extrachromosomal multicopy arrays containing copies of the experimental and marker plasmids. All transgenic strains were maintained and assayed at 16°C unless otherwise noted.

Phenotypic scoring

The uncoordinated phenotype was initially quantified by photographing the tracks left by single transgenic or control worms over a 40 s test period and measuring both the track and animal lengths to calculate body lengths travelled per minute (Fig. 2B). Movement deficits were routinely quantified by counting body thrashes in liquid scored under the dissecting microscope for 30 s intervals (Fig. 6B).

Nematode immunohistochemistry and immunoblotting

For immunohistochemistry, worms were fixed in 4% paraformaldehyde and permeabilized by Tris–Triton X-100/collagenase

treatment as previously described (17) and probed with either rabbit polyclonal anti-TDP-43 (ProteinTech Group anti-TARDBP, final concentration 0.53 µg/ml) or mouse monoclonal anti-TDP-43 (Abnova M01, final concentration 5 µg/ml).

For immunoblotting (Fig. 1D and Supplementary Material, Fig. S1), 70 transgenic worms were picked into 10 µl of water and snap frozen. After boiling in sample buffer (1 mM AEBSF-containing protease inhibitor cocktail, 62 mM Tris pH6.8, 2% SDS, 10% glycerol, 4% β-mercaptoethanol, 0.0005% Bromophenol blue), samples were run at 180 V on Nu PAGE 4–12% Bis–Tris Gel (Invitrogen, NP0321) using MES SDS Running Buffer (Invitrogen NP0002). Gel was transferred to 0.45 µm supported nitrocellulose (GE Osmonics WP4HY00010) using 20% methanol, 39 mM glycine, 48 mM Tris base. Transfer conditions were 35 V, 70 min. Prestained Rainbow size markers (Amersham Biosciences RPN755, RPN800) were used to size bands. Blots were visualized by Ponceau stain, then boiled for 3 min in phosphate-buffered saline (PBS). Blots were blocked in TBS-Tween + 5% milk (100 mM Tris7.5, 150 mM NaCl, 0.1% Tween-20). The blot was probed with 1 µg/ml TARDBP mouse monoclonal antibody (Abnova cat#H00023435-MO1). For reprobing the blot, actin monoclonal antibody JLA20 (Developmental Studies Hybridoma Bank, University of Iowa) was diluted 1:100 in blocking solution. Secondary HRP-conjugated antibodies (Sigma A5906 mouse) were developed in ECL Plus (Amersham RPN2132).

Quantification of neuronal defects

Synapse quantification was performed on four strains: CL1681: *juls1[unc-25::SNB-1::GFP]* IV; dvEx681[pCL256 (*snb-1::hTDP-43*; pVH13.06, *unc-122::GFP*), CL1684: *juls1[unc-25::SNB-1::GFP]* IV; dvEx684[pVH13.06, *unc-122::GFP*], CZ333: *juls1[unc-25::SNB-1::GFP]* IV and CL6155: *tdp-1(ok781)* II; *juls1[unc-25::SNB-1::GFP]* IV. Transgenic adult worms propagated at 20°C were anesthetized in M9 buffer containing 10 mM sodium azide and mounted on agar pads. For CL1681, animals displaying a severe uncoordinated phenotype were selected. Worms that displayed a dorsal view were imaged along their entire dorsal cord by spinning disc confocal microscopy. Dorsal cord identification and imaging was initiated using the DsRed2 signal provided by the pVH13.06 (*rgef-1/DsRed2*) marker, thus acquisition of the GFP synapse marker images was observer blind.

Cell counts of GABAergic motor neurons were performed using CL6139: *hdlIs22 (unc-129/CFP; unc-47/DeRed2)* V; *dvIs62* [pCL256(*snb-1/hTDP-43*) + pCL26(*mtl-2/GFP*)] X and control strain VH577: *hdlIs22 (unc-129/CFP; unc-47/DsRed2)* V. Fourth larval stage worms grown at 16°C were anesthetized in 0.1% tricane + 0.01% tetramisole, mounted on agar pads and scored by DIC and epifluorescence microscopy using a Zeiss Axioskop equipped with an 100× oil immersion lens. DsRed-marked cell bodies in the ventral cord were scored; only unambiguous cell bodies were counted. Worms from both strains were mounted on the same slide and scored with the observer blind to genotype (subsequently determined by presence or absence of GFP in the intestine). Although *C. elegans* has 19 GABAergic motor neurons, counts in control (and experimental) groups were slightly less than 19,

presumably due to the occasional inability to distinguish individual cell bodies in closely opposed pairs of neurons.

Microscopy

General immunofluorescence and GFP images were acquired with a Zeiss Axioskop equipped with a 100 W Xenon bulb and a digital deconvolution system (Intelligent Imaging Innovations). Images shown in Figure 2C and 4A, and all panels in Figure 7, are single planes from digitally deconvoluted optical stacks (1 μm steps), with image contrast and brightness digitally adjusted in Photoshop. (Fig. 4I is a projection image of 6 deconvoluted sections.)

For the characterization of dorsal cord axonal and synapse morphology, images were acquired using a Zeiss Axioplan II equipped with a Quorum WaveFX spinning disc confocal system (Yokagawa CSU10 head). A 491 nm laser was used for GFP excitation and a 561 nm laser for DsRed excitation. Images were collected using a 40 \times /1.3 Oil immersion PlanApo-chromat lens and a Hamamatsu Oera ER camera. Image stacks with 0.2 μm vertical pitch and 0.158 μm lateral resolution were collected sequentially for the GFP and DsRed channels. Laser intensity and exposure times were kept constant for all animals.

Cell culture transfection and immunocytochemistry

HEK293 cells, grown on glass cover slips, were transfected with 0.3 μg of expression vector (GFP-TDP-43, untagged TDP-43, TDP-43-Myc or Flag-TDP-43) by using Lipofectamine 2000 (Invitrogen) according to the manufacturer's instructions and then subjected to immunofluorescence analysis 48 h later. The cultured HEK293 cells were fixed with 4% paraformaldehyde in PBS at 4°C for 15 min and permeabilized with PBS–0.5% Triton X-100 for 10 min. After blocking with 5% BSA for 1 h at 37°C, the cells were incubated overnight at 4°C with rabbit polyclonal TDP-43 antibody (1:2000; ProteinTech), mouse monoclonal myc antibody (1:2000, Roche Applied Science) or mouse monoclonal Flag antibody (1:1000, Sigma). After washing, cells were incubated with the Alexa 568-conjugated goat anti-mouse IgG secondary antibody (1:1000, Molecular Probes) or anti-rabbit IgG secondary antibody (1:1000, Molecular Probes) at 37°C for 2 h. Finally, Hoechst 33258 (1 $\mu\text{g}/\text{ml}$, Invitrogen) was used to stain the nuclei. Images were obtained on a Zeiss LSM 510 META confocal microscope.

Cell toxicity assay

M17 neuroblastoma cells, seeded at 1.5×10^4 cells per well in six-well plates, were grown in Neurobasal A/B27 medium containing Glutamax (Invitrogen) and 10 μM retinoic acid (Sigma) to induce differentiation. Seven days later, cells were transfected with 1 μg of expression vector for 72 h. The medium was collected and a LDH assay (Promega) was used to measure LDH levels as an indicator of toxicity. Then, cells were harvested for western blot.

Cell culture immunoblots

The differentiated M17 cells were harvested in lysis buffer (50 mM Tris–HCl, pH 7.4, 1 M NaCl, 1% Triton X-100,

5 mM EDTA) plus 1% SDS, PMSF and both a protease and phosphatase inhibitor mixture. Protein concentrations of cells lysates were measured by BCA assay (Thermo Scientific). Samples were prepared in Laemmli's buffer, heated for 5 min at 95°C, and equal amounts of protein were loaded into 10-well 10% Tris-glycine gels (Novex). After transfer, blots were blocked with 5% non-fat dry milk in TBST (tris-buffered saline plus 0.1% Triton X-100) for 1 h, and then the blots were incubated with rabbit polyclonal anti-TDP-43 antibody (1:2000; ProteinTech) overnight at 4°C. Membranes were washed three times for 10 min in TBST and then incubated with donkey anti-rabbit IgG conjugated to horseradish peroxidase (1:5000; Jackson ImmunoResearch) for 1 h. Membranes were washed three times each for 10 min, and protein expression was visualized by ECL treatment and exposure to film. Protein bands were quantitatively analyzed by Multi Gauge software (Fujifilm) and were expressed as sum optical density. TDP-43 protein levels were normalized to GAPDH. Finally, all of them were expressed as relative level against corresponding control.

Cell-based assay for CFTR alternative splicing

The procedure described in D'Ambrogio *et al.* (37) was used to compare the ability of hTDP-43 and TDP-1 to support CFTR alternative splicing. Briefly, HeLa cells were plated at 30% of confluence (day 0) and two rounds of TDP-43 siRNA transfections were carried out according to the procedure already described (38) on days 1 and 2 in order to maximize TDP-43 silencing efficiency. Transfection of 0.5 μg of the CFTR C155T reporter minigene (39) together with 1 μg of pFLAG-expressed proteins was performed on day 3. Cells were harvested on day 4 and total RNA was collected with Trizol Reagent (Invitrogen). Reverse transcription was performed using M-MLV Reverse Transcriptase (Invitrogen), according to the manufacturer's protocol. PCR with DNA Polymerase (Roche) was carried out for 35 amplification cycles (95°C for 30 s, 55°C for 30 s, 72°C for 30 s). PCR products were analyzed on 1.5% agarose gels.

For experiments examining the activity of TDP-43 deletion and fusion variants (Fig. 8, no siRNA), HeLa cells were cultured in standard laboratory conditions. The (TG)₁₃(T)₅ CFTR splicing assay was used as described previously (39). HeLa six-well plate co-transfections were performed with 1 μg (TG)₁₃(T)₅ CFTR minigene and 1 μg pEGFP C1 vector only or carrying TDP-43, worm *tdp-1*, TDP-43.aa76–414, the hybrid construct TDP-43.aa1–270::*tdp-1*.aa347–411 or TDP-43.aa1–257. Transfected cells were grown for 48 h before checking on an inverted fluorescent microscope for expression. Cells were then harvested, washed in PBS and split into two. One aliquot was prepared for RNA with (Qiagen) RNeasy kit. One microgram of RNA was used for cDNA synthesis (SuperScript III First-Strand Synthesis System, Invitrogen). Two microliters of cDNA was assayed for splicing of exon 9 by PCR of regions flanking CFTR minigene, followed by gel electrophoresis (13). Densitometric intensity of bands was determined using MetaMorph software. Percent inclusion exon in minigene was determined as the proportion of the highest running band out of all the amplified material. The second cell aliquot was prepared for immunoblot

analysis as described above and probed using rabbit monoclonal anti-GFP (1:2000; Invitrogen), mouse monoclonal anti-TDP-43 (1:2000; Abnova), rabbit polyclonal anti-TDP-1 (made in house) and mouse monoclonal anti-GAPDH (1:10000; BioDesign).

SUPPLEMENTARY MATERIAL

Supplementary Material is available at *HMG* online.

ACKNOWLEDGEMENTS

We would like to thank Hannah Elena Schwartz for initial characterization of transgenic strains, Andrea Lynne Hall for phenotypic analysis and Justin Springett and Vishantie Sudama for media preparation. Some nematode strains were provided by the *Caenorhabditis* Genetics Center, funded by the NIH National Center for Research Resources. The JLA20 monoclonal antibody was obtained from the Developmental Studies Hybridoma Bank developed under the auspices of the NICHD.

Conflict of Interest statement. None declared.

FUNDING

This work was supported by Mayo Clinic Foundation (L.P.), the National Institutes of Health/National Institute on Aging [R01AG026251 and P01-AG17216-08 (L.P.)], the National Institutes of Health/National Institute of Neurological Disorders and Stroke [R01 NS 063964-01 (L.P.) and R01 NS063964 (C.D.L.)], the Amyotrophic Lateral Sclerosis Association (L.P.), the Department of Defense USAMRMC PR080354 (L.P.), the Canadian Institutes of Health Research (H.H.), the Michael Smith Foundation for Health Research (H.H.) and AriSLA (E.B.).

NOTE ADDED IN PROOF

While this manuscript was under revision, another transgenic *Drosophila* model of TDP-43 toxicity was described [Hanson, K. A., Kim, S. H., Wassarman, D. A., and Tibbetts, R. S. (2010) Ubiquitin modifies TDP-43 toxicity in a *Drosophila* model of amyotrophic lateral sclerosis (ALS). *J. Biol. Chem.* **285**, 11068–11072.], in which nuclear accumulation of wild type TDP-43 was found to be neurotoxic.

REFERENCES

- Ou, S.H., Wu, F., Harrich, D., Garcia-Martinez, L.F. and Gaynor, R.B. (1995) Cloning and characterization of a novel cellular protein, TDP-43, that binds to human immunodeficiency virus type 1 TAR DNA sequence motifs. *J. Virol.*, **69**, 3584–3596.
- Buratti, E. and Baralle, F.E. (2001) Characterization and functional implications of the RNA binding properties of nuclear factor TDP-43, a novel splicing regulator of CFTR exon 9. *J. Biol. Chem.*, **276**, 36337–36343.
- Strong, M.J., Volkening, K., Hammond, R., Yang, W., Strong, W., Leystra-Lantz, C. and Shoemaker, C. (2007) TDP43 is a human low molecular weight neurofilament (hNFL) mRNA-binding protein. *Mol. Cell Neurosci.*, **35**, 320–327.
- Arai, T., Hasegawa, M., Akiyama, H., Ikeda, K., Nonaka, T., Mori, H., Mann, D., Tsuchiya, K., Yoshida, M., Hashizume, Y. and Oda, T. (2006) TDP-43 is a component of ubiquitin-positive tau-negative inclusions in frontotemporal lobar degeneration and amyotrophic lateral sclerosis. *Biochem. Biophys. Res. Commun.*, **351**, 602–611.
- Neumann, M., Sampathu, D.M., Kwong, L.K., Truax, A.C., Micsenyi, M.C., Chou, T.T., Bruce, J., Schuck, T., Grossman, M., Clark, C.M. *et al.* (2006) Ubiquitinated TDP-43 in frontotemporal lobar degeneration and amyotrophic lateral sclerosis. *Science*, **314**, 130–133.
- Mackenzie, I.R. and Rademakers, R. (2008) The role of transactive response DNA-binding protein-43 in amyotrophic lateral sclerosis and frontotemporal dementia. *Curr. Opin. Neurol.*, **21**, 693–700.
- Amador-Ortiz, C., Lin, W.L., Ahmed, Z., Personett, D., Davies, P., Duara, R., Graff-Radford, N.R., Hutton, M.L. and Dickson, D.W. (2007) TDP-43 immunoreactivity in hippocampal sclerosis and Alzheimer's disease. *Ann. Neurol.*, **61**, 435–445.
- Nakashima-Yasuda, H., Uryu, K., Robinson, J., Xie, S.X., Hurtig, H., Duda, J.E., Arnold, S.E., Siderowf, A., Grossman, M., Leverenz, J.B. *et al.* (2007) Co-morbidity of TDP-43 proteinopathy in Lewy body related diseases. *Acta Neuropathol.*, **114**, 221–229.
- Geser, F., Martinez-Lage, M., Robinson, J., Uryu, K., Neumann, M., Brandmeir, N.J., Xie, S.X., Kwong, L.K., Elman, L., McCluskey, L. *et al.* (2009) Clinical and pathological continuum of multisystem TDP-43 proteinopathies. *Arch. Neurol.*, **66**, 180–189.
- Ayala, Y.M., Pantano, S., D'Ambrogio, A., Buratti, E., Brindisi, A., Marchetti, C., Romano, M. and Baralle, F.E. (2005) Human, *Drosophila*, and *C.elegans* TDP43: nucleic acid binding properties and splicing regulatory function. *J. Mol. Biol.*, **348**, 575–588.
- Davidson, Y., Kelley, T., Mackenzie, I.R., Pickering-Brown, S., Du Plessis, D., Neary, D., Snowden, J.S. and Mann, D.M. (2007) Ubiquitinated pathological lesions in frontotemporal lobar degeneration contain the TAR DNA-binding protein, TDP-43. *Acta Neuropathol.*, **113**, 521–533.
- Zhang, Y.J., Xu, Y.F., Dickey, C.A., Buratti, E., Baralle, F., Bailey, R., Pickering-Brown, S., Dickson, D. and Petrucelli, L. (2007) Progranulin mediates caspase-dependent cleavage of TAR DNA binding protein-43. *J. Neurosci.*, **27**, 10530–10534.
- Zhang, Y.J., Xu, Y.F., Cook, C., Gendron, T.F., Roettges, P., Link, C.D., Lin, W.L., Tong, J., Castanedes-Casey, M., Ash, P. *et al.* (2009) Aberrant cleavage of TDP-43 enhances aggregation and cellular toxicity. *Proc. Natl Acad. Sci. USA*, **106**, 7607–7612.
- Igaz, L.M., Kwong, L.K., Chen-Plotkin, A., Winton, M.J., Unger, T.L., Xu, Y., Neumann, M., Trojanowski, J.Q. and Lee, V.M. (2009) Expression of TDP-43 C-terminal fragments *in vitro* recapitulates pathological features of TDP-43 proteinopathies. *J. Biol. Chem.*, **284**, 8516–8524.
- Igaz, L.M., Kwong, L.K., Xu, Y., Truax, A.C., Uryu, K., Neumann, M., Clark, C.M., Elman, L.B., Miller, B.L., Grossman, M. *et al.* (2008) Enrichment of C-terminal fragments in TAR DNA-binding protein-43 cytoplasmic inclusions in brain but not in spinal cord of frontotemporal lobar degeneration and amyotrophic lateral sclerosis. *Am. J. Pathol.*, **173**, 182–194.
- Kabashi, E., Lin, L., Tradewell, M.L., Dion, P.A., Bercier, V., Bourgouin, P., Rochefort, D., Bel Hadj, S., Durham, H.D., Vande Velde, C., Rouleau, G.A. and Drapeau, P. Gain and loss of function of ALS-related mutations of TARDBP (TDP-43) cause motor deficits. *in vivo. Hum. Mol. Genet.*, **19**, 671–683.
- Link, C.D. (1995) Expression of human beta-amyloid peptide in transgenic *Caenorhabditis elegans*. *Proc. Natl Acad. Sci. USA*, **92**, 9368–9372.
- Faber, P.W., Alter, J.R., MacDonald, M.E. and Hart, A.C. (1999) Polyglutamine-mediated dysfunction and apoptotic death of a *Caenorhabditis elegans* sensory neuron. *Proc. Natl Acad. Sci. USA*, **9**, 179–184.
- Kraemer, B.C., Zhang, B., Leverenz, J.B., Thomas, J.H., Trojanowski, J.Q. and Schellenberg, G.D. (2003) Neurodegeneration and defective neurotransmission in a *Caenorhabditis elegans* model of tauopathy. *Proc. Natl Acad. Sci. USA*, **100**, 9980–9985.
- Hallam, S.J. and Jin, Y. (1998) *lin-14* regulates the timing of synaptic remodelling in *Caenorhabditis elegans*. *Nature*, **395**, 78–82.
- Sakamoto, R., Byrd, D.T., Brown, H.M., Hisamoto, N., Matsumoto, K. and Jin, Y. (2005) The *Caenorhabditis elegans* UNC-14 RUN domain

- protein binds to the kinesin-1 and UNC-16 complex and regulates synaptic vesicle localization. *Mol. Biol. Cell*, **16**, 483–496.
22. Nakata, K., Abrams, B., Grill, B., Goncharov, A., Huang, X., Chisholm, A.D. and Jin, Y. (2005) Regulation of a DLK-1 and p38 MAP kinase pathway by the ubiquitin ligase RPM-1 is required for presynaptic development. *Cell*, **120**, 407–420.
 23. Grill, B., Bienvenut, W.V., Brown, H.M., Ackley, B.D., Quadroni, M. and Jin, Y. (2007) *C. elegans* RPM-1 regulates axon termination and synaptogenesis through the Rab GEF GLO-4 and the Rab GTPase GLO-1. *Neuron*, **55**, 587–601.
 24. Hengartner, M.O. and Horvitz, H.R. (1994) Programmed cell death in *Caenorhabditis elegans*. *Curr. Opin. Genet. Dev.*, **4**, 581–586.
 25. Link, C.D., Taft, A., Kapulkin, V., Duke, K., Kim, S., Fei, Q., Wood, D.E. and Sahagan, B.G. (2003) Gene expression analysis in a transgenic *Caenorhabditis elegans* Alzheimer's disease model. *Neurobiol. Aging*, **24**, 397–413.
 26. Buratti, E., Brindisi, A., Giombi, M., Tisminetzky, S., Ayala, Y.M. and Baralle, F.E. (2005) TDP-43 binds heterogeneous nuclear ribonucleoprotein A/B through its C-terminal tail: an important region for the inhibition of cystic fibrosis transmembrane conductance regulator exon 9 splicing. *J. Biol. Chem.*, **280**, 37572–37584.
 27. Link, C.D., Fonte, V., Hiester, B., Yerg, J., Ferguson, J., Csontos, S., Silverman, M.A. and Stein, G.H. (2006) Conversion of green fluorescent protein into a toxic, aggregation-prone protein by C-terminal addition of a short peptide. *J. Biol. Chem.*, **281**, 1808–1816.
 28. Wu, Y., Wu, Z., Butko, P., Christen, Y., Lambert, M.P., Klein, W.L., Link, C.D. and Luo, Y. (2006) Amyloid-beta-induced pathological behaviors are suppressed by Ginkgo biloba extract EGb 761 and ginkgolides in transgenic *Caenorhabditis elegans*. *J. Neurosci.*, **26**, 13102–13113.
 29. McIntire, S.L., Jorgensen, E. and Horvitz, H.R. (1993) Genes required for GABA function in *Caenorhabditis elegans*. *Nature*, **364**, 334–337.
 30. Gould, T.W., Buss, R.R., Vinsant, S., Prevette, D., Sun, W., Knudson, C.M., Milligan, C.E. and Oppenheim, R.W. (2006) Complete dissociation of motor neuron death from motor dysfunction by Bax deletion in a mouse model of ALS. *J. Neurosci.*, **26**, 8774–8786.
 31. Ayala, Y.M., Zago, P., D'Ambrogio, A., Xu, Y.F., Petrucelli, L., Buratti, E. and Baralle, F.E. (2008) Structural determinants of the cellular localization and shuttling of TDP-43. *J. Cell. Sci.*, **121**, 3778–3785.
 32. Johnson, B.S., McCaffery, J.M., Lindquist, S. and Gitler, A.D. (2008) A yeast TDP-43 proteinopathy model: Exploring the molecular determinants of TDP-43 aggregation and cellular toxicity. *Proc. Natl Acad. Sci. USA*, **105**, 6439–6444.
 33. Li, Y., Ray, P., Rao, E.J., Shi, C., Guo, W., Chen, X., Woodruff, E.A. III, Fushimi, K. and Wu, J.Y. A *Drosophila* model for TDP-43 proteinopathy. *Proc. Natl Acad. Sci. USA*, **107**, 3169–3174.
 34. Wils, H., Kleinberger, G., Janssens, J., Pereson, S., Joris, G., Cuij, I., Smits, V., Ceuterick-de Groote, C., Van Broeckhoven, C. and Kumar-Singh, S. (2010) TDP-43 transgenic mice develop spastic paralysis and neuronal inclusions characteristic of ALS and frontotemporal lobar degeneration. *Proc. Natl Acad. Sci. USA*, **107**, 3858–3863.
 35. Wegorzewska, I., Bell, S., Cairns, N.J., Miller, T.M. and Baloh, R.H. (2009) TDP-43 mutant transgenic mice develop features of ALS and frontotemporal lobar degeneration. *Proc. Natl Acad. Sci. USA*, **106**, 18809–18814.
 36. Nonet, M.L., Saifee, O., Zhao, H., Rand, J.B. and Wei, L. (1998) Synaptic transmission deficits in *Caenorhabditis elegans* synaptobrevin mutants. *J. Neurosci.*, **18**, 70–80.
 37. D'Ambrogio, A., Buratti, E., Stuani, C., Guarnaccia, C., Romano, M., Ayala, Y.M. and Baralle, F.E. (2009) Functional mapping of the interaction between TDP-43 and hnRNP A2 *in vivo*. *Nucleic Acids Res.*, **37**, 4116–4126.
 38. Mercado, P.A., Ayala, Y.M., Romano, M., Buratti, E. and Baralle, F.E. (2005) Depletion of TDP 43 overrides the need for exonic and intronic splicing enhancers in the human apoA-II gene. *Nucleic Acids Res.*, **33**, 6000–6010.
 39. Pagani, F., Buratti, E., Stuani, C. and Baralle, F.E. (2003) Missense, nonsense, and neutral mutations define juxtaposed regulatory elements of splicing in cystic fibrosis transmembrane regulator exon 9. *J. Biol. Chem.*, **278**, 26580–26588.
 40. Brandt, R., Gergou, A., Wacker, I., Fath, T. and Hutter, H. (2009) A *Caenorhabditis elegans* model of tau hyperphosphorylation: induction of developmental defects by transgenic overexpression of Alzheimer's disease-like modified tau. *Neurobiol. Aging*, **30**, 22–33.